Talanta 97 (2012) 533–538

Contents lists available at SciVerse ScienceDirect

Talanta

journal homepage: www.elsevier.com/locate/talanta

Micrococcal nuclease detection based on peptide-bridged energy transfer between quantum dots and dye-labeled DNA

Yanhong Chen [a], Lei Wang [b], Wei Jiang [a,*]

[a] School of Chemistry and Chemical Engineering, Shandong University, 250100 Jinan, PR China
[b] School of Pharmacy, Shandong University, 250012 Jinan, PR China

ARTICLE INFO

Article history:
Received 24 March 2012
Received in revised form
3 May 2012
Accepted 8 May 2012
Available online 15 May 2012

Keywords:
Fluorescence resonance energy transfer
Quantum dots
Peptide
Electrostatic interaction
Micrococcal nuclease

ABSTRACT

A novel and simple method was presented for micrococcal nuclease (MNase) detection based on fluorescence resonance energy transfer (FRET) realized by electrostatic interaction. In this study, mercaptoacetic acid capped quantum dots (MAA-QDs) and ROX-modified single-stranded DNA (ROX-ssDNA) were chosen as energy donor and acceptor, respectively. At slightly basic pH, the positively charged peptide served as a bridge to bring negatively charged QDs and negatively charged ROX-ssDNA into close contact to energy transfer. When the ROX-ssDNA was cleaved into small fragments by MNase, the relatively weak electrostatic interaction between the fragmented ssDNA chains and the QDs/peptide complex should make the ROX away from the QDs/peptide complex, and thus the FRET efficiency decreased. Consequently, the fluorescence intensity of acceptor decreased and a quantification of the MNase was enabled. Under the optimal conditions, experimental results showed that the fluorescence intensity of acceptor was proportional to the logarithm of MNase concentration in a range of 4.0×10^{-3}–8.0×10^{-2} U mL^{-1}. The proposed approach offered adequate sensitivity for the detection of the MNase at 2.9×10^{-3} U mL^{-1}.

1. Introduction

Nucleases play vital roles in biological processes, such as DNA replication, repair and recombination. They are also considered to be necessary tools in PCR assay, genotyping, molecular cloning and medicinal chemistry [1–5]. As a result, the detection of nucleases is important for modern molecular biology and drug discovery. Traditional methods, including gel electrophoresis [6–8], radioactive labeling [9] and enzyme-linked immunosorbent assay (ELISA) [10], have been reported. Most of them are time-consuming, laborious, and require sophisticated instrumentation or isotope labeling. To address these limitations, fluorescence assays based on fluorescence resonance energy transfer (FRET) technology have been applied and developed because of their intrinsic high sensitivity and selectivity, among which molecular beacons and conjugated polymers have often been used in nuclease detection assays [11–15]. However, these strategies are compromised to expensive double fluorophore-labeled DNA substrates and complicated synthesis procedure, unlocalized emission, polydispersity of conjugated polymers [16]. Thus development of a simple and sensitive method for nuclease analysis should be of general interest.

Recently, as a kind of promising fluorescent nanomaterial, quantum dots (QDs) have received much attention. QDs possess unique optical and electronic characteristics compared with organic fluorophores, such as superior photostability, high quantum yields, broad absorption spectra, and narrow emission spectra [17–19]. Therefore, QDs as excellent energy donors have been reported for detecting nucleases [20–22]. Gill et al. designed QDs/dye-DNA duplex structure to monitor the cleavage of the DNA by DNase I [20]. Huang et al. developed an exonuclease detection method using QDs/ssDNA-fluorescent dye conjugates as biosensor [21]. Suzuki et al. presented FRET-based QDs bioprobe to detect the actions of deoxyribonuclease and DNA polymerase [22]. However, these approaches need double-labeled DNA probes and covalent immobilization of the probe DNA to the QDs surface, which often add to the cost and complexity.

Constructing QDs/DNA FRET system through electrostatic interaction is emerging as an alternative to covalent binding. This strategy is simple and requires no covalent immobilization of the probe DNA. Besides, the nature of electrostatic interaction can ensure the probe DNA coming into close proximity of QDs to obtain a high FRET efficiency [23]. Peng et al. first designed a simple sensing platform for DNA hybridization based on electrostatic interaction, taking advantage of the cationic polymer mediated QDs-FRET system [24]. Subsequently, Jiang et al. established a cascaded FRET system, in which the fluorescent conjugated polymer acted not only as a bridge but also as a light-harvesting

* Corresponding author. Tel.: +86 531 88363888; fax: +86 531 88564464.
E-mail address: wjiang@sdu.edu.cn (W. Jiang).

0039-9140/$ - see front matter © 2012 Elsevier B.V. All rights reserved.
http://dx.doi.org/10.1016/j.talanta.2012.05.010

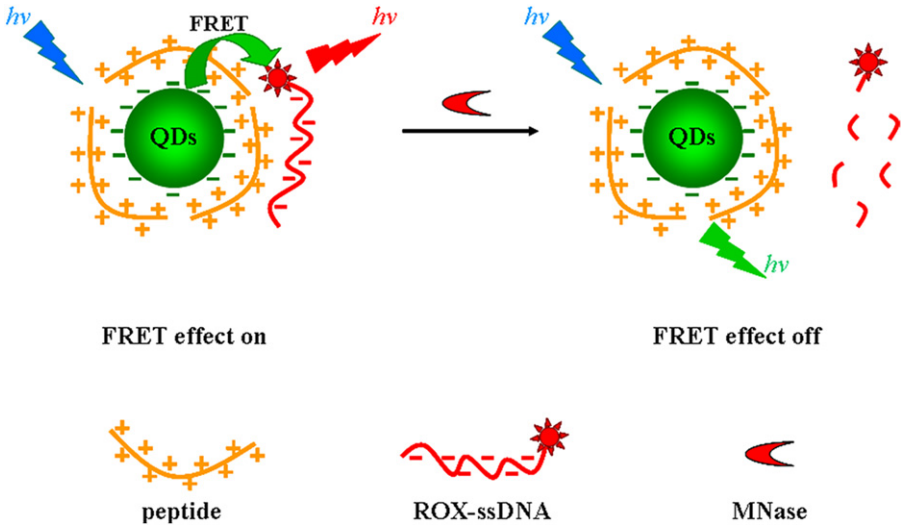

Fig. 1. Schematic description of the assay for MNase detection.

antenna [25]. Recently, He et al. reported a QDs-based FRET probe for nuclease detection by means of the electrostatic principle [26]. But, this method still involved a modification process to get positively charged QDs via two-step conjugation reaction, and the process was complicated and time-intensive.

Herein, we developed a novel and simple method for micrococcal nuclease (MNase) detection based on QDs-FRET system through peptide acting as an electrostatic linker. The MNase is an endo-exonuclease which could preferentially digest single-stranded DNA at AT-rich regions at slightly basic pH [27]. As shown in Fig. 1, the positively charged peptides electrostatically self-assembled on the surface of the negatively charged QDs to form a positively charged QDs/peptide complex. Then the complex could attract negatively charged ROX-ssDNA for energy transfer. In the presence of MNase, the ROX-ssDNA was cut into fragments, the FRET efficiency decreased due to the weak interaction between QDs and the small DNA fragments, thus providing a sensing platform for MNase. This approach was simple in design, and labor-intensive QDs covalent modification was avoided. The quantification of the MNase was successfully accomplished with a detection limit of 2.9×10^{-3} U mL^{-1}.

2. Experimental

2.1. Reagents

The mercaptoacetic acid capped CdSe/ZnS quantum dots (MAA-QDs) was commercially purchased from Wuhan Jiayuan Quantum Dots Co., Ltd. (Wuhan, China). The peptide (sequence Arg-Arg-Arg-Arg-Arg-Arg-Arg-Arg-Arg-Arg) was synthesized from the GenScript Biotechnology Corporation (Nanjing, China) and used without further purification. All of oligonucleotides were synthesized by Sangon Biotech Co., Ltd. (Shanghai, China), and their base sequences in detail were as follows: 5-mer, 5′-ROX-TAT AT-3′, 10-mer, 5′-ROX-TAT ATG GAT G-3′, 20-mer, 5′-ROX-TAT ATG GAT GAT GTG GTA TT-3′. Micrococcal nuclease, Exonuclease III (Exo III) and S1 nuclease were obtained from TaKaRa (Dalian, China). Thrombin was purchased from Dingguo Biological Technology Corporation (Beijing, China). Pepsin was obtained from Solarbio Science and Technology Co., Ltd. (Beijing, China). Other reagents and chemicals were analytical grade and used as received. Tris–HCl buffer (pH=9.0) containing 2.0×10^{-2} mol L^{-1} Tris–HCl, 5.0×10^{-3} mol L^{-1} NaCl and 2.5×10^{-3} mol L^{-1} $CaCl_2$ was used throughout the experiment. All solutions were prepared using ultrapure water (18.2 MΩ cm) by standard methods.

2.2. Apparatus

All the fluorescence measurements were performed on an F-4500 spectrofluorimeter (Hitachi, Tokyo, Japan).

The pH was acquired on a Lei Ci PHS-3C pH-meter (Shanghai, China).

2.3. Methods

2.3.1. Peptide-bridged energy transfer between QDs and ROX-ssDNA

2.0 μL 4.0×10^{-6} mol L^{-1} ROX-ssDNA solution was mixed with 1.0 μL 5.0×10^{-6} mol L^{-1} QDs and 2.0 μL 1.0×10^{-4} mol L^{-1} peptide in 95 μL Tris–HCl buffer (pH=9.0). And then, the mixture was kept for 5 min and moved to a fluorescence cuvette for fluorescence measurement.

2.3.2. FRET-based nuclease assay

95 μL Tris–HCl buffer (pH=9.0) contained different amounts of MNase and ROX-ssDNA (8.0×10^{-8} mol L^{-1}, final concentration). The above solution was incubated at 37 °C for MNase-catalyzed reaction. After a specific incubation time, the cleaved ROX-ssDNA solution was cooled to room temperature, then, 1.0 μL 5.0×10^{-6} mol L^{-1} QDs solution and 2.0 μL 1.0×10^{-4} mol L^{-1} peptide solution were added to react with the cleaved ROX-ssDNA product. The mixture was kept for 5 min and followed by fluorescence measurement.

All samples were illuminated at an excitation wavelength of 400 nm, and the fluorescence emission was recorded from 500 to 650 nm. The excitation and emission slit widths were 10 nm.

3. Results and discussion

3.1. Peptide-bridged energy transfer between QDs and ROX-ssDNA

MAA-QDs were negatively charged at slightly basic environment. A 20-mer ROX-labeled ssDNA containing AT-rich regions was used as the probe ssDNA to recognize and detect MNase. The peptide consisting of ten arginine units was designed as an electrostatic linker. The isoelectric point of arginine was around 10.76 [28], which suggested that the peptide had positive charges

in the Tris–HCl buffer (pH=9.0). Acting as a medium, the peptide could bring the QDs and ROX-ssDNA together through electrostatic binding to form the QDs/peptide/ROX-ssDNA complex. In this complex the QD served as a FRET donor to transfer energy to ROX acceptor. Fig. S1 in Supporting Information showed their normalized absorption and emission spectra. The emission spectrum of the QDs had a good spectral overlap with the absorption spectrum of ROX, which indicated that FRET between them could take place. The broad absorption band of QD allowed sample excitation at 400 nm without direct excitation of ROX. In addition, there was minimal spectral cross-talk between the QDs and ROX emissions, satisfying the requirement for effective separation of fluorescence emission of donor and acceptor. The absorption and emission spectra of QDs after the binding of the peptide were also studied. As shown in Fig. S1, both the absorption and emission spectra of QDs and QDs/peptide complex showed negligible changes in the peak emission wavelength and bandwidth, which indicated that the grafting of peptide did not affect the optical properties of QDs.

To verify the occurrence of FRET between the QDs and ROX in the QDs/peptide/ROX-ssDNA complex, the fluorescence spectra of different systems were studied (Fig. 2). Curve a and b were the fluorescence spectra of ROX-ssDNA and QDs/peptide, respectively. It was obvious that QDs were powerfully excited while the interference from acceptor direct emission was effectively reduced upon excitation at 400 nm. Curve c corresponds to the fluorescence spectrum of QDs/ROX-ssDNA. Because of slight hydrogen-bonding interactions between carboxylic acid ligands and DNA nucleobases [29], negligible energy was transferred from negatively charged QDs to ROX-ssDNA. However, in the presence of the peptide, the fluorescence intensity of QDs was significantly weakened with the obvious enhancement of the ROX fluorescence intensity (curve d). By comparison with curve c, it was found that an effective FRET occurred with the addition of peptide, suggesting that the electrostatic interaction played a key role to ensure the energy transfer between the QD donor and the ROX acceptor. A control experiment was performed to study whether ssDNA without the ROX label could affect the QDs fluorescence. Under the same conditions as used above, the QDs/peptide complex was incubated with the ssDNA without the ROX label, the quenching of the QDs fluorescence was less than 5% (curve e).

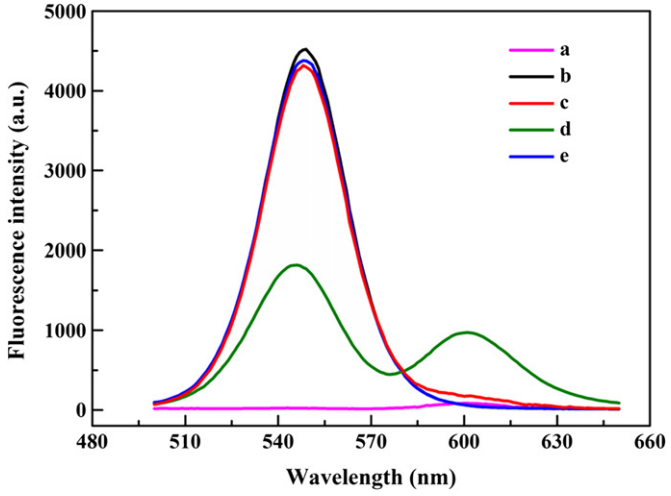

Fig. 2. Fluorescence emission spectra of FRET systems. (a) ROX-ssDNA, (b) QDs/peptide, (c) QDs/ROX-ssDNA, (d) QDs/peptide/ROX-ssDNA, (e) QDs/peptide/ssDNA. Condition: QDs: 5.0×10^{-8} mol L^{-1}, peptide: 2.0×10^{-6} mol L^{-1}, ROX-ssDNA and ssDNA: 8.0×10^{-8} mol L^{-1}.

3.2. Effect of peptide concentration

The peptide was employed as an "electrostatic linker" to provide a positively charged surface, allowing negatively charged ROX-ssDNA to interact with the resulting complex. In order to obtain high FRET efficiency, the effect of peptide concentration was investigated. The fluorescence response was studied using the fluorescence intensity of ROX at 600 nm as standard. As illustrated in Fig. 3, the initial additions of peptide caused an immediate rise in the fluorescence signal of ROX, reached a plateau when the peptide concentration was up to 2.0×10^{-6} mol L^{-1}. A possible reason was that, the surface positive charge density of the QDs/peptide complex gradually rose as the peptide concentration increased, therefore more ROX-ssDNA molecules would bind to the complex and the transferred energy was enhanced. When the peptide concentration reached 2.0×10^{-6} mol L^{-1}, the surface positive charge of the QDs/peptide complex approached saturation. In this case, the amount of the ROX-ssDNA absorbed to the surface of the QDs/peptide complex did not change, so the signal kept relatively stable. The effect of the peptide concentration on the fluorescence intensity of ROX could further prove that the peptide served as the electrostatic medium for FRET between negative QDs and negative ROX-ssDNA. Finally, 2.0×10^{-6} mol L^{-1} was chosen as the optimal peptide concentration.

3.3. Effect of ROX-ssDNA

Firstly, 5-mer, 10-mer, 20-mer ROX-ssDNA chains at the same concentration were selected to study the influence of oligonucleotide length on the FRET efficiency. As shown in Fig. 4A, the fluorescence intensity of ROX gradually increased with increasing length of ssDNA from 5 to 20 mer. The result showed that the change of the fluorescence signal of ROX was due to the variety of the chain length of the ssDNA. The result was understandable by considering the fact that the enhancement of electrostatic interaction between the QDs/peptide complex and the longer ssDNA because long DNA had higher charge density than that of short DNA, resulting in an increase in FRET efficiency. It is well known that the ssDNA can be cleaved into fragments by nuclease. Therefore, it was possible to employ the FRET system to perform the nuclease cleavage assay. In this work, 20-mer ROX-ssDNA was selected as the substrate of the MNase digestion reaction.

Furthermore, to obtain the best fluorescence signal, the concentration of ROX-ssDNA (20-mer) was tested. As seen in Fig. 4B,

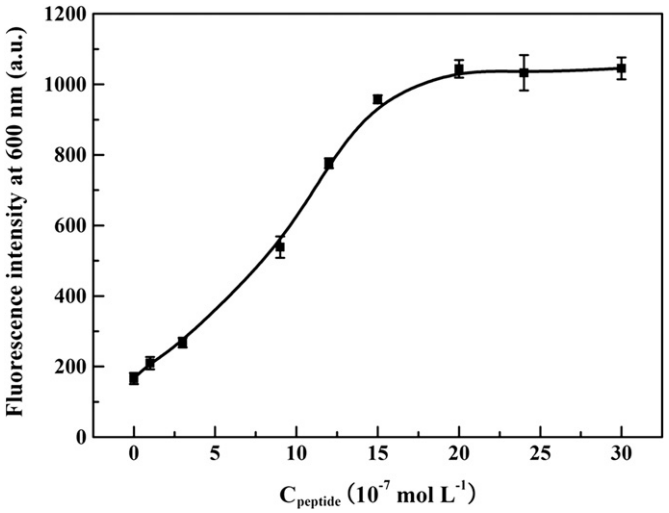

Fig. 3. Effect of peptide concentration on the fluorescence intensity of ROX. Condition: QDs: 5.0×10^{-8} mol L^{-1}, ROX-ssDNA: 8.0×10^{-8} mol L^{-1}.

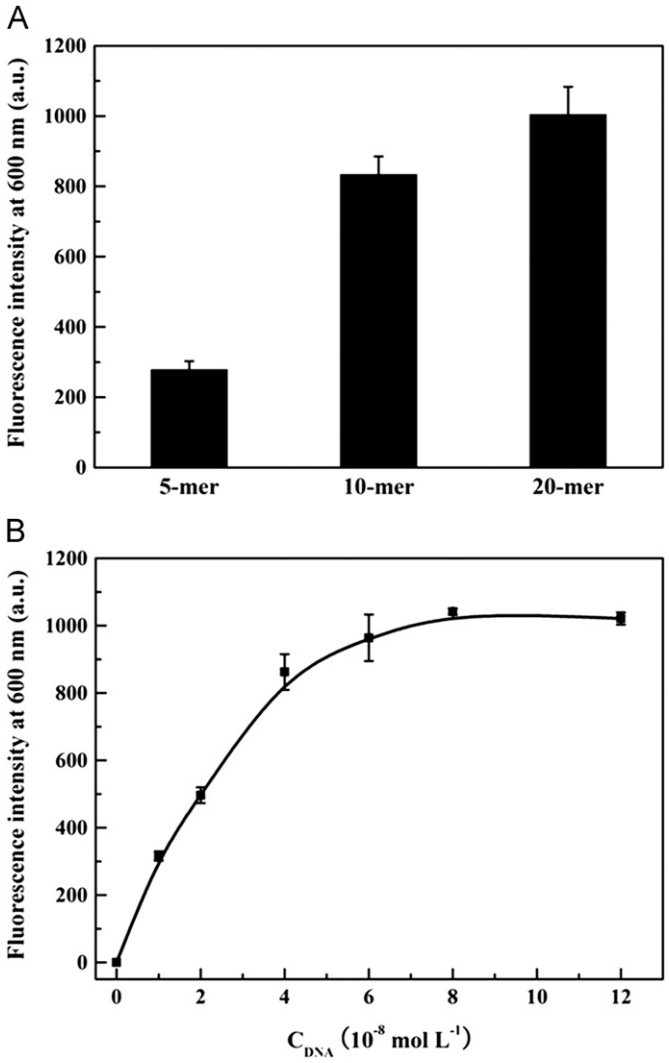

Fig. 4. (A) Effect of the ROX-ssDNA length on the fluorescence intensity of ROX. Condition: QDs: 5.0×10^{-8} mol L^{-1}, peptide: 2.0×10^{-6} mol L^{-1}, ROX-ssDNA: 8.0×10^{-8} mol L^{-1}. (B) Effect of ROX-ssDNA (20-mer) concentration on the fluorescence intensity of ROX. Condition: QDs: 5.0×10^{-8} mol L^{-1}, peptide: 2.0×10^{-6} mol L^{-1}.

the fluorescence intensity of ROX enhanced according to the increase of the ROX-ssDNA concentration. Because the surface of the QDs/peptide complex was saturated with the ROX-ssDNA molecules, then the signal reached a steady state at the concentration up to 8.0×10^{-8} mol L^{-1}. Therefore, the ROX-ssDNA concentration was selected at 8.0×10^{-8} mol L^{-1} throughout the study.

3.4. Effect of pH

To confirm the charge-based QDs/peptide/ROX-DNA complex formation, Tris–HCl buffer samples with different pH values were conducted to investigate the effect of pH in the complex formation. As given in Fig. S2 in Supporting Information, the maximum fluorescence intensity of ROX was observed for pH between 8.0 and 9.0, with less intensity for lower or higher pH conditions. The possible reason was that, the formation of less protonated carboxylic acid groups on the surface of QDs at lower pH and the less charged peptide in the high pH region reduced the electrostatic interaction between the QDs and peptide. Therefore, maximum energy transfer was achieved when both the QDs and the peptide were charged, which more ROX-ssDNA molecules were absorbed to the positively charged surface of the QDs/peptide complex. The result suggested that the FRET system was susceptible to the influence of pH, confirming the realization of QDs/peptide/ROX-DNA complex was based upon the electrostatic interaction. Besides, the pH of media was chosen as 9.0.

3.5. Effect of Ionic strength

Not only the pH but also the ionic strength would interfere with the electrostatic interaction, so the effect of ionic strength on the complex formation was also evaluated by increasing the NaCl concentration of Tris–HCl buffer (pH=9.0). As shown in Fig. S3 in Supporting Information, when the NaCl concentration was lower than 4.0×10^{-2} mol L^{-1}, the electrostatic potential between the QDs and peptide was enough to bring the two together, thus providing a positively charged surface to attract ROX-ssDNA. When the NaCl concentration was up to 4.0×10^{-2} mol L^{-1}, the increase of the NaCl concentration resulted in a drop in the energy transfer between QDs and ROX. On the basis of the Debye-Hückel theory, the addition of NaCl screened the surface charge of QDs, which weakened the electrostatic interaction between the QDs and peptide of opposite charge, so the surface charge density of QDs/peptide complex decreased. Then the number of ROX-ssDNA absorbed to the surface of QDs/peptide complex declined and the FRET between QDs and ROX got weak. 5.0×10^{-3} mol L^{-1} NaCl was employed in the study.

3.6. Stability test of QDs/peptide/ROX-ssDNA system

The stability of the QDs/peptide/ROX-ssDNA system was tested under the optimal conditions. The tendency to change of fluorescence intensity of ROX was measured at different time and the result was presented in Fig. S4 in Supporting Information. As it can be seen, the fluorescence intensity of ROX enhanced rapidly and tended to a maximum value at 2 min, indicating a fast rate of electrostatic reaction, and then changed little within 2–10 min. After 10 min, the fluorescence signal decreased slightly by extending the reaction time. In this method, the QDs/peptide/ROX-ssDNA complex was kept for 5 min followed by fluorescence measurement.

3.7. FRET-based MNase assay

3.7.1. Detection of MNase

Under optimized conditions, the QDs/peptide/ROX-DNA complex was applied to detect the MNase. At a fixed concentration of MNase (8.0×10^{-2} U mL^{-1}), the changes in fluorescence spectra of the complex as a function of MNase digestion time was monitored. As shown in Fig. 5, with MNase digestion, the emission intensity at 600 nm from ROX gradually decreased and the emission from QDs at 548 nm showed a gradual increase over the incubating time from 0 to 30 min. This indicated that the strength of electrostatic interaction between QDs/peptide and ROX-ssDNA reduced over digestion time due to the small ssDNA fragmentation, which increased the distance between QDs/peptide and ROX, resulting in inefficient FRET between them.

Fig. 6 revealed the time curves of the intensity of ROX at 600 nm with various MNase concentrations from 4.0×10^{-3} to 8.0×10^{-2} U mL^{-1}. Obviously, the intensity of ROX decreased at each MNase concentration by prolonging the cleavage reaction time, which was followed by a plateau. In addition, increasing the concentration of MNase gave rise to a faster enzymatic reaction rate and a higher level of fluorescence decrease of ROX. In other words, if the concentration of the ROX-ssDNA substrate in the cleavage reaction solution was fixed, the cleavage reaction rate was dependent on the concentration of the MNase. After the ROX-ssDNA was digested for 50 min at 37 °C, the fluorescence intensity of ROX at 600 nm was recorded to detect MNase. As shown in

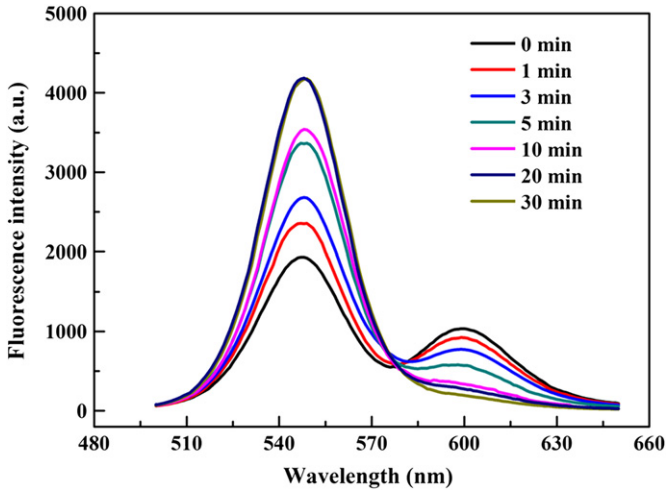

Fig. 5. Fluorescence emission spectra of QDs/peptide/ROX-ssDNA complex as a function of MNase digestion. Condition: QDs: 5.0×10^{-8} mol L^{-1}, peptide: 2.0×10^{-6} mol L^{-1}, ROX-ssDNA: 8.0×10^{-8} mol L^{-1}, and MNase: 8.0×10^{-2} U mL^{-1}.

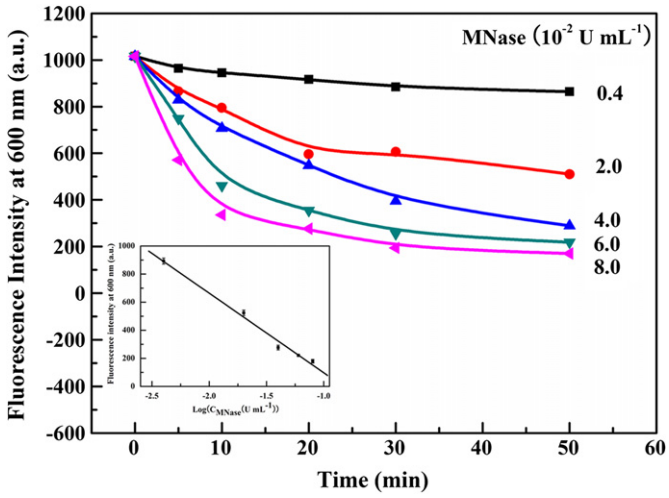

Fig. 6. The time-dependent ROX fluorescence intensity as a function of digestion time with varying MNase concentration. Inset: The linear relationship between ROX fluorescence intensity and the logarithm of MNase concentration. Condition: QDs: 5.0×10^{-8} mol L^{-1}, peptide: 2.0×10^{-6} mol L^{-1}, and ROX-ssDNA: 8.0×10^{-8} mol L^{-1}.

Fig. 6 (inset), a linear relationship was observed between the fluorescence intensity of ROX at 600 nm and the logarithm of MNase concentration in a dynamic range from 4.0×10^{-3} to 8.0×10^{-2} U mL^{-1}. The linear regression equation was determined to be $Y=-468.5-566.2\log[C_{MNase}]$ with the correlation coefficient of 0.9940. The detection limit of MNase was 2.9×10^{-3} U mL^{-1} (3 times the standard deviation above the blank), which had a comparable detection limit compared with the methods mentioned above [21,26].

3.7.2. *The selectivity of MNase assay*

To determine the selectivity of this assay for MNase, a series of experiments were carried out using MNase and other common proteins including Exonuclease III (Exo III), S1 nuclease, thrombin and pepsin. As demonstrated in Fig. 7, In contrast to the blank, only the MNase exhibited a remarkable decrease in fluorescence intensity at 600 nm. Under the same conditions, the other enzymes failed to induce significant fluorescence decrease. Therefore, it can be considered that the decrease of fluorescence intensity arose from the ROX-ssDNA cleavage by its specific MNase, demonstrating the high selectivity of this system for MNase.

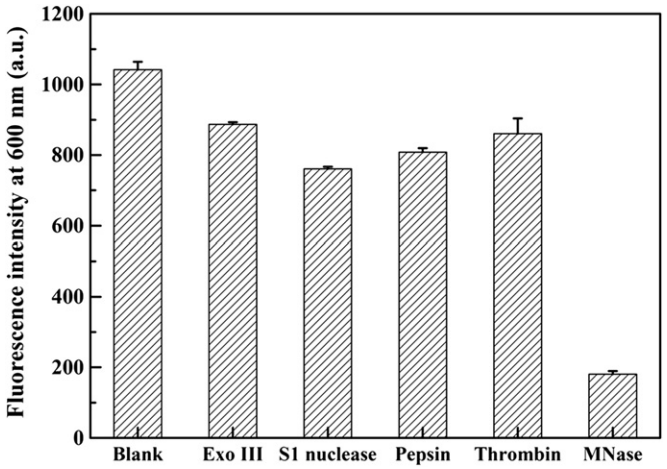

Fig. 7. The selectivity of this FRET system toward MNase over other common enzymes. Condition: QDs: 5.0×10^{-8} mol L^{-1}, peptide: 2.0×10^{-6} mol L^{-1}, ROX-ssDNA: 8.0×10^{-8} mol L^{-1}, MNase: 8.0×10^{-2} U mL^{-1}, Exo III=S1 nuclease: 2.0 U mL^{-1}, and thrombin=pepsin: 2.5×10^{-7} mol L^{-1}.

4. Conclusions

In summary, we have demonstrated a novel and simple MNase detection strategy based on the FRET. The ROX-ssDNA was connected to the MAA-QDs for energy transfer via an electrostatic interaction in the presence of a peptide linker. The presence of the MNase led to the degradation of the DNA sequence, the different electrostatic interaction strength of ssDNA and fragments with the QDs/peptide complex caused different changes of FRET efficiency, thus allowing for the MNase detection. This assay utilized the electrostatic interaction to realize the FRET. Compared with previous reports, this method was simplified, easy to operate, and offered comparable sensitivity as previously reported FRET analysis for MNase detection. In addition, neither covalent modification to the QDs nor doubly labeled DNA strand was required, leading to the development of a low cost and less laborious method. Furthermore, this method could be extended to detect other nucleases which are active at slightly basic pH by changing the substrate DNA.

Acknowledgments

This project was supported by the National Natural Science Foundation of China (Grant Nos. 21175081, 21175082) and the Natural Science Foundation of Shandong Province in China (Grant No. Z2008B05).

Appendix A. Supporting information

Supplementary data associated with this article can be found in the online version at http://dx.doi.org/10.1016/j.talanta.2012.05.010.

References

[1] W. Arber, Angew. Chem. Int. Ed. 17 (1978) 73–79.
[2] M.R. Lieber, Bioessays 19 (1997) 233–240.
[3] R.J. Roberts, Nucleic Acids Res. 18 (1990) 2331–2365.
[4] T.M. Marti, O. Fleck, Cell Mol. Life Sci. 61 (2004) 336–354.

[5] P. Norberg, T. Bergstrom, J.A. Liljeqvist, J. Clin. Microbiol. 44 (2006) 4511–4514.
[6] A.L. Rosenthal, S.A. Lacks, Anal. Biochem. 80 (1977) 76–90.
[7] T. Karpetsky, G.E. Brown, E. McFarland, S.T. Brady, W. Roth, A. Rahman, P. Jewett, Biochem. J. 219 (1984) 553–561.
[8] K.M.M. Miyahara, Anal. Chim. Acta 213 (1988) 273–277.
[9] G.S. Boswell, S.D. Dimitrijevich, R.W. Gracy, Anal. Biochem. 182 (1989) 20–24.
[10] A. Jeltsch, A. Fritz, J. Alves, H. Wolfes, A. Pingoud, Anal. Biochem. 213 (1993) 234–240.
[11] C. Ma, Z. Tang, X. Huo, X. Yang, W. Li, W. Tan, Talanta 76 (2008) 458–461.
[12] C. Ma, Z. Tang, K. Wang, W. Tan, X. Yang, W. Li, Z. Li, X. Lv, Anal. Biochem. 363 (2007) 294–296.
[13] F. Pu, D. Hu, J. Ren, S. Wang, X. Qu, Langmuir 26 (2010) 4540–4545.
[14] Y. Zhang, Y. Wang, B. Liu, Anal. Chem. 81 (2009) 3731–3737.
[15] X. Feng, X. Duan, L. Liu, F. Feng, S. Wang, Y. Li, D. Zhu, Angew. Chem. Int. Ed. 48 (2009) 5316–5321.
[16] K.E. Sapsford, L. Berti, I.L. Medintz, Angew. Chem. Int. Ed. 45 (2006) 4562–4589.
[17] M. Bruchez Jr., M. Moronne, P. Gin, S. Weiss, A.P. Alivisatos, Science 281 (1998) 2013–2016.
[18] I.L. Medintz, H.T. Uyeda, E.R. Goldman, H. Mattoussi, Nat. Mater. 4 (2005) 435–446.
[19] W.R. Algar, U.J. Krull, Anal. Chem. 82 (2010) 400–405.
[20] R. Gill, I. Willner, I. Shweky, U. Banin, J. Phys. Chem. B 109 (2005) 23715–23719.
[21] S. Huang, Q. Xiao, Z.K. He, Y. Liu, P. Tinnefeld, X.R. Su, X.N. Peng, Chem. Commun. (2008) 5990–5992.
[22] M. Suzuki, Y. Husimi, H. Komatsu, K. Suzuki, K.T. Douglas, J. Am. Chem. Soc. 130 (2008) 5720–5725.
[23] J. Lee, Y. Choi, J. Kim, E. Park, R. Song, ChemPhysChem 10 (2009) 806–811.
[24] H. Peng, L. Zhang, T.H. Kjallman, C. Soeller, J. Travas-Sejdic, J. Am. Chem. Soc. 129 (2007) 3048–3049.
[25] G. Jiang, A.S. Susha, A.A. Lutich, F.D. Stefani, J. Feldmann, A.L. Rogach, ACS Nano 3 (2009) 4127–4131.
[26] T. Qiu, D. Zhao, G. Zhou, Y. Liang, Z. He, Z. Liu, X. Peng, L. Zhou, Analyst 135 (2010) 2394–2399.
[27] T.M. Martensen, E.R. Stadtman, Proc. Nat. Acad. Sci. USA 79 (1982) 6458–6460.
[28] Q. Gao, W. Xu, Y. Xu, D. Wu, Y. Sun, F. Deng, W. Shen, J. Phys. Chem. B 112 (2008) 2261–2267.
[29] W.R. Algar, U.J. Krull, J. Colloid Interface Sci. 359 (2011) 148–154.